1521-0111/12/8104-598–609$25.00
MOLECULAR PHARMACOLOGY
Vol. 81, No. 4
76745/3759371

Mol Pharmacol 81:598–609, 2012

Regulation of Breast Cancer Resistant Protein by Peroxisome Proliferator-Activated Receptor α in Human Brain Microvessel Endothelial Cells

Md. Tozammel Hoque, Kevin R. Robillard, and Reina Bendayan

Graduate Department of Pharmaceutical Sciences, Leslie Dan Faculty of Pharmacy, University of Toronto, Toronto, Ontario, Canada

Received November 13, 2011; accepted January 19, 2012

ABSTRACT

Breast cancer resistance protein (BCRP/ABCG2), an ATP-binding cassette (ABC) membrane-associated drug efflux transporter, is known to localize at the blood-brain barrier (BBB) and can significantly restrict xenobiotic permeability in the brain. The objective of this study is to investigate the regulation of BCRP functional expression by peroxisome proliferator-activated receptor alpha (PPARα), a ligand-activated transcription factor primarily involved in lipid metabolism, in a cerebral microvascular endothelial cell culture system (hCMEC/D3), representative of human BBB. We demonstrate that PPARα-selective ligands (i.e., clofibrate, GW7647) significantly induce BCRP mRNA and protein expression in a time- and concentration-dependent manner, whereas pharmacological inhibitors (i.e., MK886, GW6471) prevent this induction. Using [^{3}H]mitoxantrone, an established BCRP substrate, we observe a significant reduction in its cellular accumulation by monolayer cells treated with clofibrate, suggesting increased BCRP efflux activity. In addition, we show a significant decrease in BCRP protein expression and function when PPARα is down-regulated by small interfering RNA. Applying chromatin immunoprecipitation and quantitative real-time polymerase chain reaction, we observe that clofibrate treatment increases PPARα binding to the peroxisome proliferator response element within the *ABCG2* gene promoter. This study provides the first evidence of direct BCRP regulation by PPARα in a human in vitro BBB model and suggests new targeting strategies for either improving drug brain bioavailability or increasing neuroprotection.

Introduction

The blood-brain barrier (BBB) localized at the interface of the systemic circulation and brain parenchyma can significantly restrict the permeability of xenobiotics including several pharmacological agents in the central nervous system (CNS) (Pardridge, 2010). In addition to the physical barrier formed by the microvessel endothelial cells, drug penetration into the brain is highly regulated by a biochemical barrier mainly constituted of metabolic enzymes and influx/efflux transport proteins (Abbott et al., 2010). In particular, the membrane-associated efflux drug transporters, breast cancer resistance protein (BCRP) and P-glycoprotein (P-gp), ex-

This work was supported by the Canadian Institutes of Health Research [Grant MOP56976] and the Ontario HIV Treatment Network, Ministry of Health of Ontario [Grant ROGB189] (to R.B.). R.B. is a career scientist of the Ontario HIV Treatment Network, Ministry of Health of Ontario. K.R. is a recipient of an Ontario HIV Treatment Network doctoral studentship award.

This work was previously presented in part at the following meeting: Hoque MT, Robillard KR, and Bendayan R (2011) Regulation of breast cancer resistant protein (BCRP) by peroxisome proliferator-activated receptor alpha (PPARα) in human brain microvessel endothelial cells, *9th International Conference on Cerebral Vascular Biology*; 2011 June 21–25, Leiden, Netherlands; International Brain Barriers Society, Duluth, MN, USA.

Article, publication date, and citation information can be found at http://molpharm.aspetjournals.org.

http://dx.doi.org/10.1124/mol.111.076745.

ABBREVIATIONS: BBB, blood-brain barrier; CNS, central nervous system; ABC, ATP-binding cassette; BCRP, breast cancer resistance protein; RXR, retinoid X receptor; P-gp, P-glycoprotein; PPARα, peroxisome proliferator-activated receptor α; PPRE, peroxisome proliferator response element; PPARγ, peroxisome proliferator-activated receptor γ; hCMEC/D3, human cerebral microvessel endothelial cells; DMSO, dimethyl sulfoxide; BBB-ECs, human brain-derived microvascular endothelial cells; siRNA, small interfering RNA; GW7647, 2-methyl-2-[[4-[2-[[(cyclohexylamino)carbonyl](4-cyclohexylbutyl)amino]-ethyl]phenyl]thio]-propanoic acid; GW6471, [(2*S*)-2-[[(1*Z*)-1-methyl-3-oxo-3-[4-(trifluoromethyl)phenyl]-1-propenyl]amino]-3-[4-[2-(5-methyl-2-phenyl-4-oxazolyl)ethoxy]phenyl]propyl]-carbamic acid ethyl ester; MK886, 1-[(4-chlorophenyl)methyl]-3-[(1,1-dimethylethyl)thio]-α, α-dimethyl-5-(1-methylethyl)-1*H*-indole-2-propanoic acid, sodium salt; MTT, (3-(4,5-dimethylthiazol-2-yl)-2,5-diphenyltetrazolium bromide; Ko143, (3*S*,6*S*,12a*S*)-1,2,3,4,6,7,12,12*a*-octahydro-9-methoxy-6-(2-methylpropyl)-1,4-dioxopyrazino[1′,2′:1,6]pyrido[3,4-*b*]indole-3-propanoic acid 1,1-dimethylethyl ester; FBS, fetal bovine serum; PBS, phosphate-buffered saline; qPCR, quantitative real-time PCR; ChIP, chromatin immunoprecipitation; PCR, polymerase chain reaction; PAGE, polyacrylamide gel electrophoresis; PVDF, polyvinylidene difluoride; DAPI, 4,6-diamidino-2-phenylindole; ANOVA, analysis of variance; ChIP, chromatin immunoprecipitation; bp, base pair(s).

pressed in brain microvessel endothelial cells, have long been recognized to play a significant role in preventing the permeability of several drugs across the BBB, presenting a great challenge to the treatment of CNS disorders (Bendayan et al., 2002, 2006; Lee et al., 2007; Ronaldson et al., 2008; Vlaming et al., 2009; Miller, 2010).

BCRP/ABCG2 belongs to the G subfamily of the ATP-binding cassette (ABC) transporter superfamily. The human *ABCG2* gene is located on chromosome 4, band 4q21–4q22, and encodes a 70-kDa, 655 amino acid protein (Polgar et al., 2008). It is known as a half-transporter that upon homodimerization exerts its functional activity. In addition to its localization at the BBB, BCRP is expressed in a wide range of tissues, including intestine, liver, kidney, testis, placenta, and mammary gland. BCRP is known to be involved in the elimination of many drugs including chemotherapeutic agents such as mitoxantrone, methotrexate, and irinotecan (Doyle et al., 1998; Maliepaard et al., 2001; Ishikawa, 2009).

Studies have examined the effect of Bcrp on cerebral drug accumulation in animal models, using established substrates, such as dantrolene or the phytoestrogens daidzein, genistein, and coumestrol. In *Abcg2* knockout mice, brain accumulation of these compounds was remarkably higher (more than 10-fold) compared with the wild-type animals (Enokizono et al., 2007, 2008).

Despite the apparent role of BCRP in protecting the brain from xenobiotic exposure, factors that regulate the expression and function of BCRP at both the gene and the protein level are poorly defined and not well understood. Investigation from our laboratory as well as other groups has implicated nuclear hormone receptors such as pregnane X receptor (PXR), constitutively active receptor, aryl hydrocarbon receptor, and estrogen receptor in the regulation of drug transporters expression and function in both human and rodent BBB models (Bauer et al., 2004, 2006; Hartz et al., 2010; Wang et al., 2010, 2011; Chan et al., 2011).

The peroxisome proliferator-activated receptor α (PPARα) belongs to the steroid hormone receptor superfamily (Robyr et al., 2000). At present, three subtypes of PPAR (α, β/δ, and γ) have been identified in many species including humans (Kersten et al., 2000). Like other steroid hormone receptors, upon ligand activation, PPARs heterodimerize with the retinoid X receptor (RXR), bind to the specific promoter sequence called the peroxisome proliferator response element (PPRE), and as a result trigger the expression of the target genes. PPRE is composed of two direct repetitions (DR1) of the consensus sequence AGGTCA with a single nucleotide spacing between the two repeats (Schachtrup et al., 2004).

PPARα is a ligand-activated transcription factor that primarily controls lipid homeostasis by regulating the expression of fatty acid metabolic enzymes (CYP4A isoforms) (Muerhoff et al., 1992). In addition, evidence suggests that PPARα could also serve as a species-specific xenosensor and regulate the expression of membrane drug efflux transporters in the liver and intestine. For example, the prototypic PPARα synthetic agonists, pirinixic acid (Wy14643), GW7647, and clofibrate, have been shown to induce the expression of Bcrp and multidrug resistant proteins 3 and 4 in mouse liver and intestine (Moffit et al., 2006; Hirai et al., 2007). However, direct molecular interaction between PPARα and Bcrp was not demonstrated.

PPARα is expressed in different compartments of rodent brain including olfactory bulbs, hippocampus, cerebellum, and cerebellar granule neurons (Cullingford et al., 1998), as well as in astrocytes (Benani et al., 2003) and microglia (Bright et al., 2008). In addition, this nuclear receptor has been reported to be expressed in human brain microvessel endothelial cells (Huang et al., 2008). However, the transcriptional activity of PPARα in the regulation of drug efflux transporters at the human BBB is currently unknown. In this study, we investigate regulation of BCRP expression and function at the BBB, using a human cerebral microvessel endothelial cell culture system (hCMEC/D3) well characterized to retain several morphological and biochemical features of the human BBB (Weksler et al., 2005). Our results demonstrate that PPARα is actively involved in the regulation of BCRP in this system. Selective modulation of BCRP expression at the BBB by PPARα can potentially lead to the development of novel therapeutic strategies for overcoming restricted drug delivery to the brain or to enhance neuroprotection.

Materials and Methods

Materials

Type I collagen was purchased from BD Biosciences (San Jose, CA). Dimethyl sulfoxide (DMSO) and acrylamide solution were obtained from Bioshop Canada Inc. (Burlington, ON, Canada). Clofibrate, 2-methyl-2-[[4-[2-[[(cyclohexylamino)carbonyl](4-cyclohexylbutyl)amino]-ethyl]phenyl]thio]-propanoic acid) (GW7647), [(2*S*)-2-[[(1*Z*)-1-methyl-3-oxo-3-[4-(trifluoromethyl)phenyl]-1-propenyl]amino]-3-[4-[2-(5-methyl-2-phenyl-4-oxazolyl)ethoxy]phenyl]propyl]-carbamic acid ethyl ester (GW6471), 1-[(4-chlorophenyl)methyl]-3-[(1,1-dimethylethyl)thio]-α,α-dimethyl-5-(1-methylethyl)-1*H*-indole-2-propanoic acid, sodium salt (MK886), 3-(4,5-dimethylthiazol-2-yl)-2,5-diphenyltetrazolium (MTT), chloroform, paraformaldehyde (37%), phenylmethylsulfonyl fluoride, (3*S*,6*S*,12a*S*)-1,2,3,4,6,7,12,12a-octahydro-9-methoxy-6-(2-methylpropyl)-1,4-dioxopyrazino[1′,2′:1,6]pyrido[3,4-*b*]indole-3-propanoic acid 1,1-dimethylethyl ester (Ko143), unlabeled mitoxantrone, anti-actin (mouse monoclonal) antibody, and protease inhibitor cocktail were all purchased from Sigma-Aldrich Canada (Mississauga, ON, Canada). Western blot stripping solution and enhanced chemiluminescent reagents were ordered from Thermo Fisher Scientific (Waltham, MA). Hybond-P polyvinylidene difluoride (PVDF) membrane and microscope cover glass slide (22 × 22 mm, thickness no. 1) were supplied from GE Healthcare Life Sciences (Piscataway, NJ) and Thermo Fisher Scientific, respectively. [^{3}H]Mitoxantrone (12.7 Ci/mmol) was ordered from Moravek Biochemicals Inc. (Brea, CA). ABI high-capacity reverse-transcriptase cDNA kit and anti-P-gp antibody were obtained from Applied Biosystems (Foster City, CA) and ID Labs Inc. (London, ON, Canada), respectively. PerfeCTa SYBR green Fastmix was purchased from Quanta Biosciences Inc. (Gaithersburg, MD). Anti-BCRP (rat monoclonal) and anti-lamin-A (mouse monoclonal) antibodies were purchased from Abcam Inc. (Boston, MA). The rabbit polyclonal anti-Na^+/K^+-ATPase-α1 antibody was purchased from Santa Cruz Biotechnology (Santa Cruz, CA). The mouse monoclonal anti-PPARα and rabbit polyclonal anti-PPARα antibodies were obtained from Perseus Proteomics Inc. (Tokyo, Japan) and Santa Cruz Biotechnology, respectively. The goat anti-mouse, anti-rat, and anti-rabbit horseradish peroxidase-conjugated secondary antibodies were ordered from Jackson ImmunoResearch Laboratories Inc. (West Grove, PA). Alexa Fluor 488- and Alexa Fluor 594-conjugated secondary antibodies, trypsin (0.25%), and the TRIzol reagent were supplied from Invitrogen (Carlsbad, CA). Vectashield mounting media containing 4,6-diamidino-2-phenylindole (DAPI) was ordered from Vector Laboratories (Burlingame, CA). Small interfering RNA (siRNA)

against PPARα (HSS108289) and nonsilencing negative control siRNA were purchased from Invitrogen and Ambion (Austin, TX), respectively.

Methods

Cell Culture Systems. The immortalized human brain microvessel endothelial cell line, hCMEC/D3, was kindly provided by Dr. P.O. Couraud (Institut Cochin, Departement Biologie Cellulaire and INSERM, Paris, France). This cell line has been widely used as a potential in vitro model of human BBB and is known to display many morphological and biochemical properties of human brain microvascular endothelium in vivo, such as functional expression of tight junction proteins, endothelial cell markers, and drug efflux transporters. Cells were used at passages 28 to 39 for all the experiments and were maintained at 37°C, 5% CO_2, and 95% humidified air in endothelial cell growth medium (Lonza Walkersville, Inc., Walkersville, MD) supplemented with vascular endothelial growth factor, insulin-like growth factor 1, epidermal growth factor, fibroblast growth factors, hydrocortisone, ascorbate, gentamicin (Lonza Walkersville, Inc.), and 2.5% fetal bovine serum (FBS). Cells were grown on rat tail collagen type I-coated 75-cm flasks, 150-cm dishes or six-well plates as described previously (Weksler et al., 2005; Zastre et al., 2009; Chan et al., 2011). Whole-cell pellets of primary cultures of human brain-derived microvascular endothelial cells (BBB-ECs) were generously provided by Dr. Alexandre Prat (Neuroimmunology Research Laboratory, Center of Excellence in Neuromics, Faculty of Medicine, Centre Hospitalier de l'Université de Montréal, Montréal, Québec, Canada). These cells were isolated from brain tissue samples obtained from young adults undergoing surgery for the treatment of intractable epilepsy and constitute an additional in vitro model of human brain microvascular endothelium. Informed consent and ethical approval were obtained from the patients before the surgery. Human fetal brain tissue (hFBT) samples were collected from consenting patients undergoing elective pregnancy termination (10–14 weeks of gestation). Ethics approval was obtained from the University Health Network (Toronto, ON, Canada). The BCRP overexpressing human breast cancer cell line, MCF7-MX100, was a generous gift from Dr. Susan Bates (Bethesda, MA). The cells were cultured and maintained in RPMI 1640 media supplemented with FBS (10%), L-glutamine (1%), penicillin (100 U/ml), streptomycin (100 μg/ml), and mitoxantrone (100 nM). The HepG2 cells were cultured in α-minimal essential medium supplemented with 10% FBS and 1% penicillin-streptomycin.

Cell Viability Assay. Cell viability in the presence of the various ligands was assessed using an MTT assay in which cells were incubated for 2 h at 37°C with a 2.5 mg/ml MTT solution in phosphate-buffered saline (PBS). The formazan content, dissolved in DMSO, from each well was determined by UV analysis at 580 nm using a SpectraMax 384 microplate reader (Molecular Devices, Sunnyvale, CA). Cell viability was expressed as the ratio between the absorbance of treated cells and the absorbance of nontreated (control) cells.

Cell Treatment. hCMEC/D3 monolayers grown on collagen-coated six-well plates, 75/175-cm flasks (approximately 80–90% confluence) were treated with PPARα ligands (clofibrate or GW7647) or PPARα antagonist (MK886/GW6471) or in combination with ligands and antagonists at specific time points (3–72 h) and concentrations (1.25 nM to 125 μM). At the beginning of each experiment, culture medium was aspirated and fresh medium containing ligands dissolved in ethanol or DMSO was added. Control cells were exposed to 0.1% (v/v) ethanol or DMSO (vehicle) in the absence of ligands. To ensure cells remain viable during treatment, all ligand concentrations used were tested applying the MTT assay as described above.

Total RNA Extraction, cDNA Synthesis and Quantitative Real-Time Polymerase Chain Reaction. Total RNA was extracted from hCMEC/D3 cells using TRIzol reagent (Invitrogen) according to manufacturer's instructions. The concentration (absorbance at 260 nm) and purity (absorbance 260 nm/absorbance 280 nm ratio) of RNA samples were assessed using a UV/Vis scanning spectrophotometer (DU Series 700; Beckman Coulter, Mississauga, ON, Canada). Isolated total RNA was subjected to DNase I digestion (0.1 U/ml) according to manufacturer's instructions to remove genomic DNA. Reverse transcription was then performed with DNase-treated total RNA (2 μg) in a final reaction volume of 40 μl using an ABI high-capacity reverse-transcription cDNA kit according to manufacturer's instructions. All sample reactions were performed at 25°C for 10 min, followed by 37°C for 120 min, and then 85°C for 5 min using Mastercycler EP Realplex 2S thermal cycler (Eppendorf Canada, Mississauga, ON, Canada). *ABCG2* and peptidylprolyl isomerase B (cyclophilin B) genes were quantified by quantitative real-time polymerase chain reaction (qPCR) on Mastercycler ep realplex 2S thermal cycler using SYBR green fluorescence detection. The 10-μl final reaction mixtures contained 1.25 μl of diluted cDNA, 5 μl of PerfeCTa SYBR Green FastMix, 0.6 μl of a 1.25 μM concentration of each primer and 2.55 μl of nuclease-free water. Specific primers were designed using Primer Express 3 (Applied Biosystems) and were on exon-exon junctions to avoid any potential amplification of genomic DNA. The specificity of each reaction was assessed by melting curve analysis to ensure the presence of only a single amplification product. Validated primer sequences are shown in Table 1. Threshold cycle (C_T) values for ABCG2 mRNA are normalized to the housekeeping gene cyclophilin B. Results are expressed as percentage change ± S.E., using a comparative C_T method ($\Delta\Delta C_T$). Changes in ABCG2 mRNA expression were calibrated to vehicle-treated cells.

siRNA Down-Regulation Studies. Cells were plated in a six-well plate with a density of 0.4×10^6 cells/well. After 24 h, cell monolayers at approximately 80% confluence were subjected to siRNA transfection. Transfection mix was prepared in Opti-MEM GlutaMax (Invitrogen) medium with siRNA and Lipofectamine 2000 (Invitrogen) according to the manufacturer's protocol. The final concentration of siRNA and Lipofectamine added to the cells were 100 nM and 2 μl/ml, respectively. Cells were cultured in the presence of transfection mixture for 24 h, as described previously (Huang et al., 2009). The following day, transfection mixture was replaced by fresh

TABLE 1
Specific qPCR forward and reverse primers

Genes and Direction	Primer Sequence (5′-3′)	Accession
ABCG2		
Forward	GGC-CTT-GGG-ATA-CTT-TGA-ATC	NM_004827
Reverse	GAA-TCT-CCA-TTA-ATG-ATG-TCC-A	
Cyclophilin B		
Forward	GGA-GAT-GGC-ACA-GGA-GGA-A	NM_000942
Reverse	GCC-CGT-AGT-GCT-TCA-GTT-T	
ABCG2 promoter (−3946/−3796)		
Forward	AGG-GCA-GAG-GGC-AAT-GG	NM_001878
Reverse	AGG-AGA-CTG-ATT-TGC-ACA-AGG-TT	
ABCG2 promoter (−1527/−1268)		
Forward	CTC-CTC-CTG-TAG-TGC-CTT-CAG-ATC-TTG-CT	NM_001878
Reverse	TTG-CAA-ATG-ACC-CGA-GAT-CCC-ACC-A	

prewarmed hCMEC/D3 medium, and cell culture was pursued for an additional 48 h. After 72 h of siRNA transfection, cells were either harvested to analyze BCRP and PPARα protein expression by immunoblotting or used for transport assays to determine mitoxantrone accumulation.

Chromatin Immunoprecipitation. Chromatin immunoprecipitation (ChIP) was performed using a ChIP assay kit and protocol provided by Affymetrix (Santa Clara, CA). In brief, hCMEC/D3 cells cultured on a 15-cm dish were treated with clofibrate (100 μM) or GW7647 (20 nM) for 3 h and subsequently cross-linked in 1% formaldehyde for 10 min at room temperature. Cross-linking was stopped by addition of glycine to a final concentration of 125 mM for 5 min at room temperature, followed by washing the cells twice in ice-cold PBS. After scrapping and centrifugation, cell pellets were suspended in 1.0 ml of lysis buffer containing protease inhibitor (Affymetrix). The chromatin was sheared to 200 to 1000 bp by sonication. The sonicated chromatin was diluted twofold in lysis buffer (Affymetrix); 600 μl of diluted sample per immunoprecipitation was used. After 1-h preclearing with protein A agarose beads (50 μl/IP), 10 μg of specific anti-PPARα antibody (Santa Cruz Biotechnology Inc.), previously validated in ChIP assays (Nagasawa et al., 2009), was added for overnight incubation. In parallel, a no-antibody sample was run as control. Protein A agarose (50 μl/IP) was used to recover the immune complexes (2 h at 4°C). Washes and elutions were performed in accordance with the ChIP assay kit. Eluted (225 μl) and input (40 μl) DNA were reverse cross-linked overnight at 65°C in the presence of 0.2 M NaCl and were purified using a spin column to a final volume of 40 μl. qPCR was performed using 2 μl of template DNA per 25 μl of polymerase chain reaction (PCR) amplification scale. Quantification of PPARα occupancy to the PPREs within the *ABCG2* gene promoter (−3946/−3796) by SYBR green real-time PCR was performed using the following primer set: forward, 5′-AGG-GCA-GAG-GGC-AAT-GG-3′ and reverse, 5′-AGG-AGA-CTG-ATT-TGC-ACA-AGG-TT-3′, which amplifies a product of 150 bp (−3946/−3796). The detection of another region (−1527/−1268) of the same *ABCG2* gene promoter, which serves as negative control, was included in similar PCRs using the following primer set: forward, 5′-CTC-CTC-CTG-TAG-TGC-CTT-CAG-ATC-TTG-CT-3′ and reverse, 5′-TTG-CAA-ATG-ACC-CGA-GAT-CCC-ACC-A-3′, which amplifies a product of 259 bp (−1527/−1268) (Table 1). Quantification was performed by qPCR (standard curve method) using serial dilutions of the input as standards. All measurements were performed in triplicate, and results were verified in at least three independent chromatin preparations.

Western Blot Analysis. Western blot analysis was performed as described previously (Zastre et al., 2009; Ronaldson et al., 2010) with minor modifications. In brief, the hCMEC/D3 monolayers, the primary cultures of human microvessel endothelial cells (BBB-ECs) and the hFBT were washed with ice-cold PBS and collected by scraping in ice-cold PBS. After centrifugation, whole-cell lysates were prepared by lysing cell pellets in lysis buffer [(1% (v/v) NP-40, 20 mM Tris, 150 mM NaCl, 5 mM EDTA at pH 7.5 containing 1 mM phenylmethylsulfonyl fluoride and 0.1% (v/v) protease inhibitor cocktail)] for 20 min at 4°C. Cell lysates were sonicated for 5 s and centrifuged at 14,000 rpm for 10 min at 4°C to remove cell debris. The whole-cell lysates were then mixed in Laemmli sample buffer and resolved on 10% SDS-polyacrylamide gel. After electrophoresis, the gels were washed in transfer buffer (25 mM Tris-HCl, pH 8, 200 mM glycine) containing 20% (v/v) methanol and then electrotransferred onto PVDF membranes. The membranes were blocked in Tris-buffered saline/Tween 20 buffer containing 5% (m/v) skim milk followed by incubation with primary antibody overnight at 4°C. The membranes were then washed in Tris-buffered saline/Tween 20 and were incubated with anti-mouse, anti-rat, or anti-rabbit horseradish peroxidase-conjugated secondary antibodies (all at 1:10,000 dilution) for 1.5 h. The BCRP protein expression was detected using a rat monoclonal anti-BCRP (1:200 dilution) antibody, which recognizes an epitope corresponding to amino acids 221 to 394 of mouse *Bcrp*.

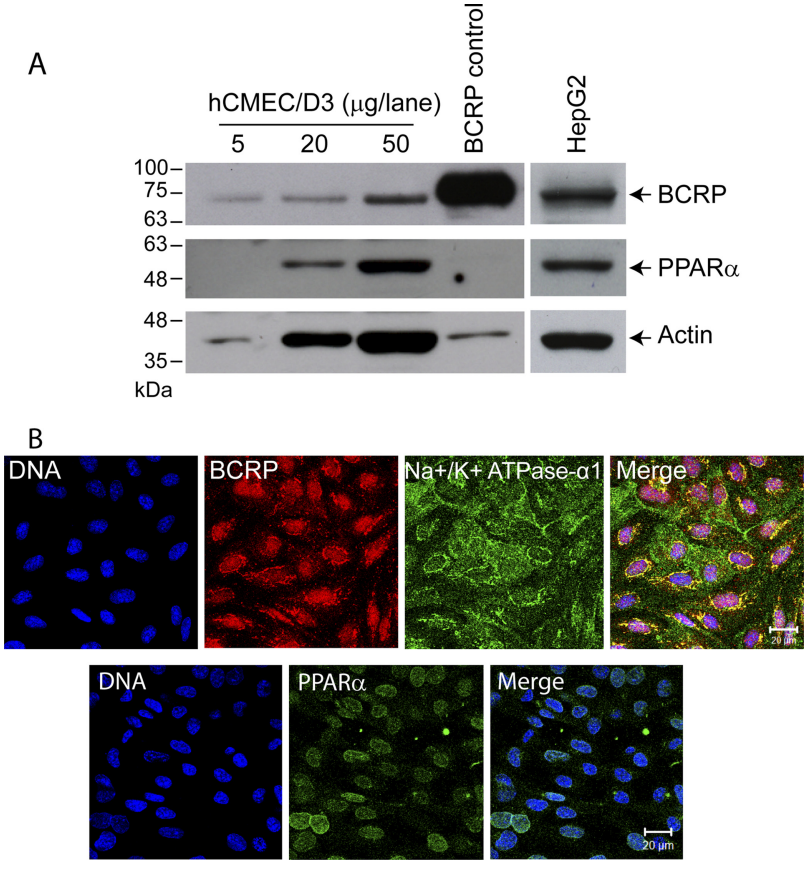

Fig. 1. Immunoblot analysis and immunocytochemical localization of BCRP and PPARα in human cerebral microvessel endothelial cells (hCMEC/D3). A, whole-cell lysates prepared from BCRP-overexpressing MCF7 MX100 (BCRP control, 5 μg), HepG2 cells (PPARα control, 50 μg), and hCMEC/D3 cells (5, 20, or 50 μg/lane) were separated on 10% SDS-polyacrylamide gel electrophoresis (PAGE) gel and subsequently transferred to PVDF membrane. The membranes were then blotted with anti-BCRP (BXP53, rat monoclonal, top), anti-PPARα (mouse monoclonal, middle), or anti-actin (AC40, mouse monoclonal, bottom) antibodies, followed by incubation with respective horseradish peroxidase conjugated anti-rat or anti-mouse secondary antibodies. B, hCMEC/D3 cells cultured on collagen-coated coverslips were fixed with ice-cold methanol and were permeabilized with 0.1% Triton X-100. Cellular localization of BCRP, Na^+/K^+-ATPase α1 and PPARα proteins were detected by mouse monoclonal anti-BCRP (1:20 dilution), rabbit polyclonal anti-Na^+/K^+-ATPase α1 (1:100 dilution), and rabbit polyclonal anti-PPARα (1:200 dilution) followed by incubation with anti-rat Alexa-594- and anti-rabbit Alexa-488-conjugated secondary antibodies (1:500 dilution/each). DNA was stained with DAPI. For negative controls, only the Alexa-conjugated secondary antibodies were used.

MCF7 MX100-overexpressing BCRP was used as a positive control. The P-gp protein expression was detected using a mouse monoclonal anti-P-gp (C219, 1:500 dilution) antibody raised against an internal epitope of human P-gp. MDA435/LCC6-MDR1 cell lysates were used as positive controls for P-gp. PPARα expression was detected using rabbit polyclonal (1:500 dilution) or mouse monoclonal (1:500 dilution) anti-PPARα antibodies, which recognize the epitopes corresponding to 4 to 96 amino acids and 1 to 98 amino acids of human PPARα protein, respectively. HepG2 cell lysates were used as positive controls for PPARα expression. Actin expression was used as loading control and was detected using mouse monoclonal AC40 antibody (1:2000 dilution). Protein bands were visualized by enhanced chemiluminescence, and protein expression was determined by densitometric analysis using Alpha DigiDoc RT2 imaging software (Alpha Innotech, San Leandro, CA).

Immunofluorescence Studies. The subcellular localization of BCRP and PPARα proteins was examined by confocal microscopy in untreated hCMEC/D3 cells, as well as in cells treated with vehicle (EtOH or DMSO) or PPARα ligands, clofibrate (100 uM), or GW7647 (20 nM) for 20 h. Cell monolayers grown on glass coverslips were fixed with 100% methanol on ice for 20 min. After fixation, cells were washed in PBS and permeabilized with 0.1% Triton X-100 for 5 min at room temperature as described previously (Hoque and Ishikawa, 2001). Fixed cells were blocked with 0.1% (m/v) bovine serum albumin and 0.1% (m/v) skim milk in PBS for 1 h before primary antibody incubation for 1.5 h at room temperature or overnight at 4°C. The rat monoclonal (BXP53, 1:20 dilution) and rabbit polyclonal (1:200 dilution) antibodies were used to detect BCRP and PPARα subcellular localization, respectively. The mouse monoclonal antibody was used to visualize lamin A expression, a marker for nuclear envelope. After primary antibody incubation, cells were washed with PBS by gentle agitation and followed by incubation with anti-mouse Alexa Fluor 594 or anti-rabbit Alexa Fluor 488 conjugated secondary antibody (both in 1:500 dilution) (Invitrogen) for 1.5 h at room temperature. Staining in the absence of primary antibodies was used as a negative control. After secondary antibody incubation, cells were washed again with PBS and mounted on a 76 $\times$ 26 mm microscope slide (VWR, West Chester, PA) using VECTASHIELD mounting solution containing DAPI. Cells were then visualized using a Plan C-Apochromat-63x/1.4 oil differential interference contrast objective and Zeiss LSM 510 META NLO two-photon confocal laser-scanning microscope (Carl Zeiss AG, Oberkochen, Germany) equipped with argon (458, 476, 488, and 513 nm wavelengths), helium-neon (533 nm wavelength), and tunable Chameleon (720–930 nm wavelengths) laser lines. Measurement of nuclear fluorescence intensity was determined using ImageJ software (ver. 1.38; http://rsb.info.nih.gov/ij). The average fluorescence intensity for each treatment group was the mean of all measurements taken from at least 100 cells.

Functional Studies. BCRP activity was measured with the use of mitoxantrone, an established substrate. Mitoxantrone accumulation by hCMEC/D3 cells was performed in Hanks' balanced salt solution, containing 1.3 mM KCl, 0.44 mM KH_2PO_4, 138 mM NaCl, 0.34 mM Na_2PO_4, and 5.6 mM D-glucose, supplemented with 0.01% bovine serum albumin and 25 mM HEPES, pH 7.4. Throughout the manuscript, supplemented Hanks' balanced salt solution buffer is referred to as transport buffer. Cells were plated at a cell density of 4×10^4 cells/cm^2, and accumulation experiments were performed at 100% cell monolayer confluence.

Cellular accumulation of [^{3}H]mitoxantrone, a known substrate of BCRP, was determined applying a radioactive transport assay as described previously (Lee et al., 2007) with slight modification. In brief, hCMEC/D3 cells were incubated with transport buffer containing 20 μM mitoxantrone ([^{3}H]mitoxantrone, 0.1 μCi/ml) in the absence or presence of the BCRP-selective inhibitor Ko143 (5 μM). After 2 h, mitoxantrone containing medium was aspirated, and cells were washed twice with ice-cold PBS and solubilized in 1% Triton X-100 at 37°C for 30 min. The content of each well was collected, mixed with 3 ml of PicoFluor 40 scintillation fluid (PerkinElmer Life

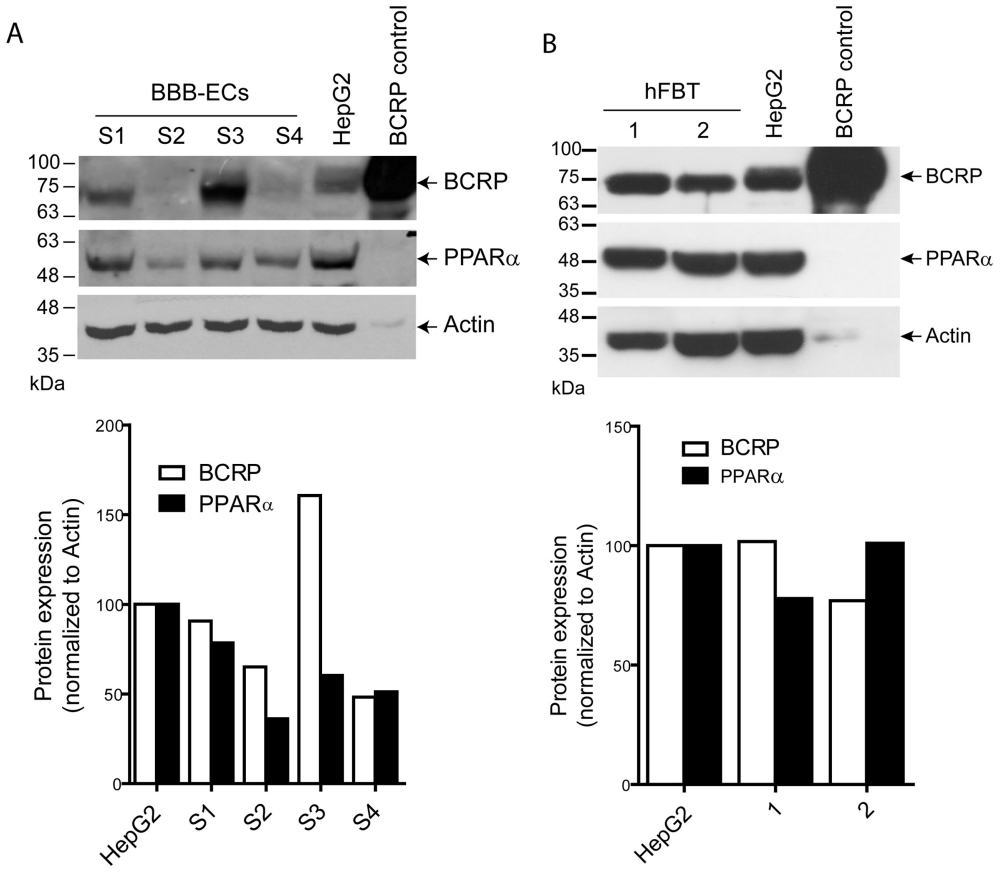

Fig. 2. Immunoblot analysis of BCRP and PPARα in primary cultures of BBB-ECs and hFBT. Whole-cell lysates prepared from human BBB-ECs pellet obtained from four individuals (S1–S4) (50 μg/each) (A) and hFBTs obtained from two individuals (1–2) (B) were resolved on a 10% SDS-PAGE gel and transferred to a PVDF membrane. HepG2 (50 μg) and MCF7 MX100 cells (5 μg) were used as positive controls for PPARα and BCRP proteins, respectively. BCRP and PPARα proteins were detected using rat and mouse monoclonal antibodies, respectively. Actin was detected using mouse monoclonal antibody (A and B). Data generated from densitometric analysis is presented as ratio of BCRP and PPARα expression normalized to actin (loading control).

and Analytical Sciences, Waltham, MA), and the total radioactivity was measured using a Beckman Coulter LS5600 liquid scintillation counter (Fullerton, CA). Background accumulation was estimated by determining the retention of radiolabeled compounds by the cells after zero time exposure, by removing the radiolabeled solution immediately after its addition into each well, followed by two subsequent washes with ice-cold PBS, and quantified using liquid scintillation counting. Total radioactive cellular accumulation was normalized to the total cellular protein content as determined by detergent-compatible protein assay (Bio-Rad Laboratories, Hercules, CA), using bovine serum albumin as the standard. For all the accumulation assays, data are reported as accumulation of the substrate at steady state in the absence or presence of inhibitor.

Statistical Analysis. All experiments were repeated at least three times in cells pertaining to different passages. Results are

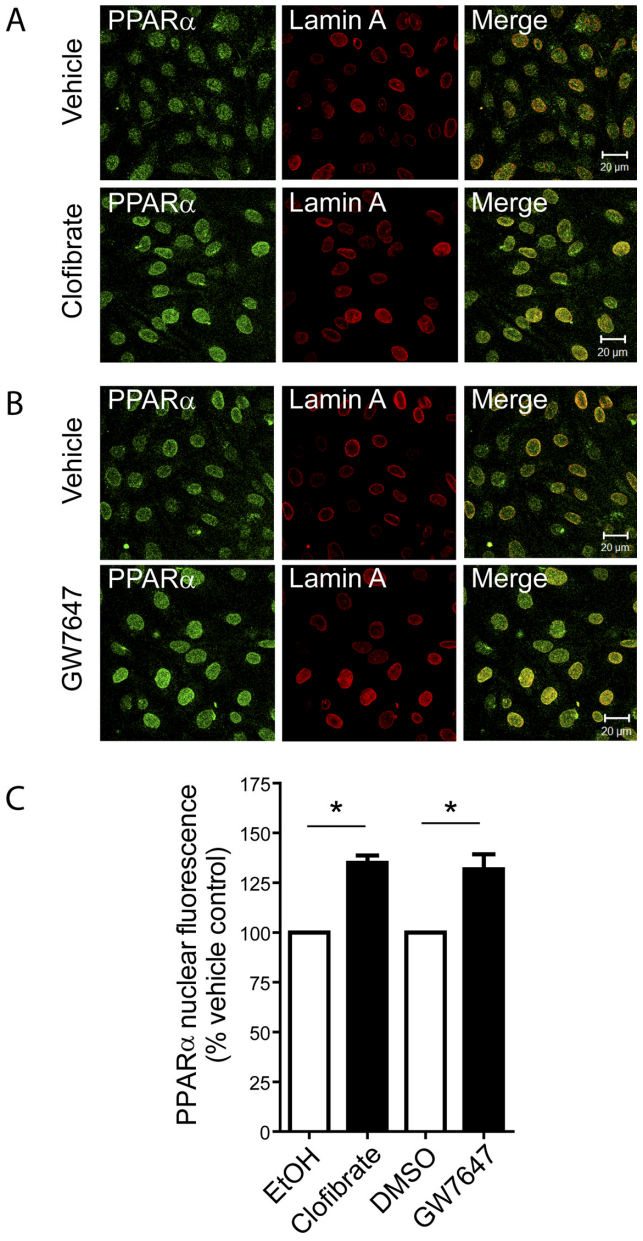

Fig. 3. Ligand-induced nuclear accumulation of PPARα in hCMEC/D3 cells. hCMEC/D3 cells grown on collagen-coated coverslips were induced with PPARα agonists, (A) clofibrate or (B) GW7647 or vehicle control (ethanol/DMSO), dissolved in hCMEC/D3 culture medium without serum for 24 h. Cells were then fixed with ice-cold methanol and permeabilized with Triton X-100 (0.1%). Cellular localization of PPARα protein was detected by rabbit polyclonal anti-PPARα antibody (1:200 dilution) followed by incubation with anti-rabbit Alexa Fluor 488-conjugated secondary antibody (1:500). Nuclear envelope was visualized with mouse monoclonal anti-Lamin-A antibody (1:500 dilution). C, average PPARα nuclear fluorescence normalized to vehicle control was obtained from three independent experiments performed in cells pertaining to different passages (>100 cells/treatment group). *, Statistically significant differences in nuclear fluorescence compared with control as determined by one-way ANOVA with Bonferroni post hoc test ($p < 0.05$).

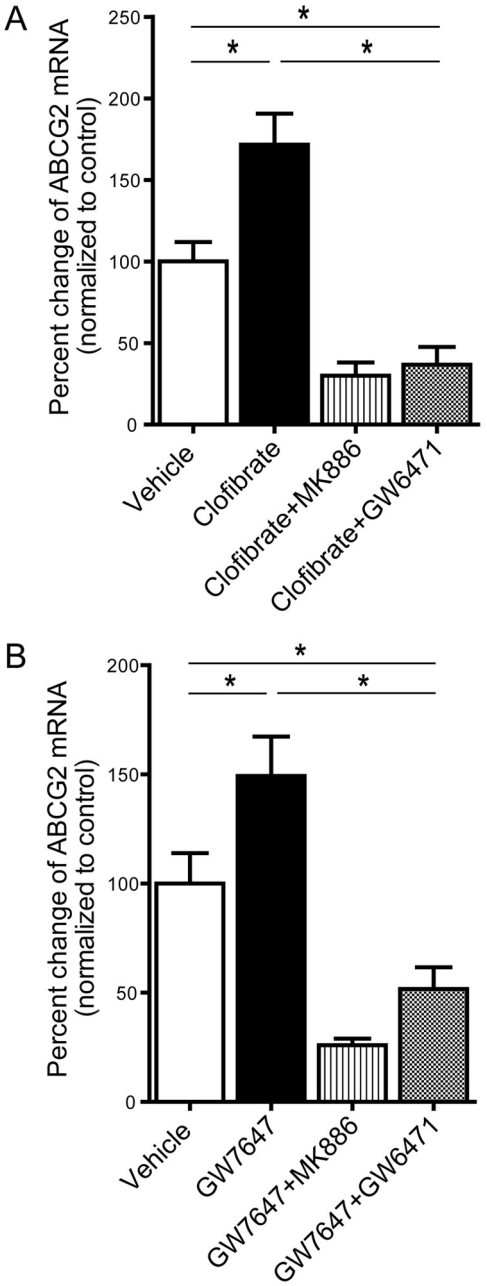

Fig. 4. Induction of ABCG2 mRNA expression by PPARα ligands in hCMEC/D3 cells. Monolayers of hCMEC/D3 cells were exposed to PPARα-selective agonists 100 μM clofibrate (A) or 20 nM GW7647 (B) or in conjunction with antagonist MK886 or GW6471 (5 μM) for 24 h. ABCG2 mRNA expression was measured by qPCR. All treatment and vehicle groups were performed in triplicate in three independent experiments pertaining to different cell passages. C_T values for ABCG2 mRNA were normalized with the housekeeping gene cyclophilin B mRNA. Results are expressed as percentage change ± S.E.M., using comparative C_T method ($\Delta\Delta C_T$). *, Statistically significant differences in ABCG2 mRNA expression compared with control as determined by one-way ANOVA with Bonferroni post hoc test ($p < 0.05$).

reported as a mean ± S.D. or as mean ± S.E. as appropriate. Comparisons between groups were performed using either two-tailed Student's t test or one-way analysis of variance (ANOVA) with Bonferroni multiple comparison post hoc test. Data were analyzed by InStat 3.0 software (Graphpad Software Inc., San Diego, CA), and a value of $p < 0.05$ was considered to be statistically significant.

Results

Expression of BCRP and PPARα Proteins in hCMEC/D3 Cells, Human BBB-ECs, and hFBTs. To document the expression of BCRP and PPARα in immortalized human cerebral microvessel endothelial cells (hCMEC/D3), primary cultures of human brain microvessel endothelial cells (BBB-ECs), and hFBTs, we performed immunoblotting analysis using whole-cell/tissue lysates with specific antibodies known to recognize BCRP and PPARα proteins, respectively. We detected BCRP and PPARα at approximately 70 and 52 kDa bands in all cell/tissue lysates examined, respectively (Figs. 1A, and 2, A and B). These are molecular mass reported previously for the two proteins (Szatmari et al., 2006; Huang et al., 2009). We observed some interindividual differences in BCRP and to a lesser extent PPARα expression in BBB-ECs (Fig. 2A). We further investigated the cellular localization of BCRP and PPARα by confocal microscopy. Anti-Na^+/K^+-ATPase α1 antibody was used as a marker of the plasma membrane. BCRP protein seemed to be primarily localized at the cell plasma membrane, whereas PPARα was found in both the nucleus and cytoplasm (Fig. 1B).

Ligand-Mediated Nuclear Accumulation of PPARα in hCMEC/D3 Cells. PPARα is a ligand-activated transcrip-

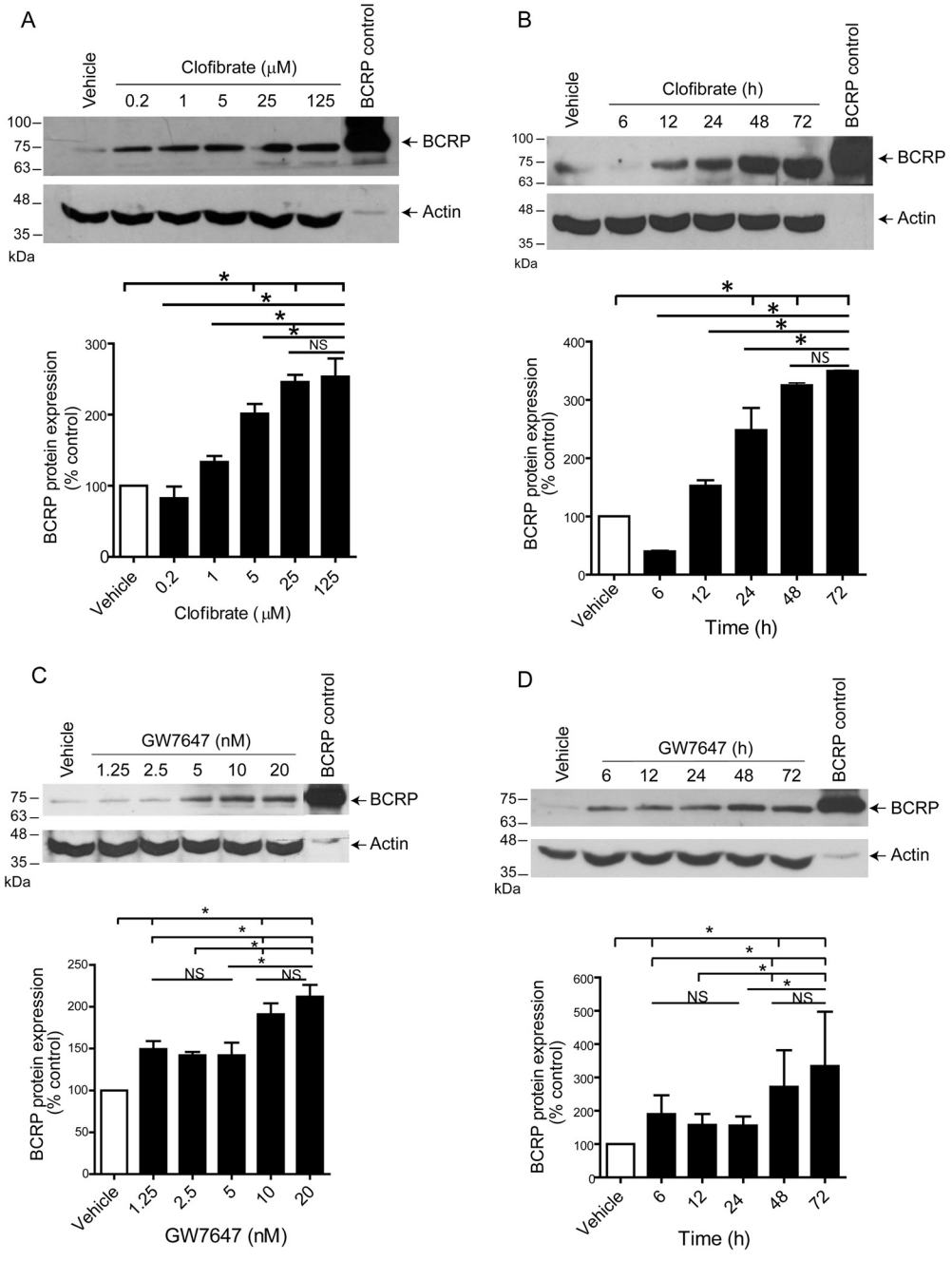

Fig. 5. Time- and concentration-dependent induction of BCRP by PPARα ligands in hCMEC/D3 cells. BCRP protein expression was measured in hCMEC/D3 cells treated with different concentrations of clofibrate (0.2–125 μM) or GW7647 (1.25–20 nM) or respective vehicle controls (ethanol/DMSO) for 72 h. A and B, representative immunoblots (top) and densitometric analyses (bottom) demonstrating the clofibrate and GW7647 concentration-dependent increase of BCRP protein expression. Quantitative densitometry analysis of three independent experiments is also shown. C and D, representative immunoblots (top) and densitometric analyses (bottom) demonstrating the clofibrate and GW7647 time-dependent increase of BCRP protein expression. The relative levels of BCRP expression were determined by densitometric analysis. Results are expressed as percentage change normalized to vehicle treated control (control) and reported as mean ± S.D. obtained from three independent experiments performed in cells pertaining to different passages. *, Statistically significant differences between treatment group as determined by one-way ANOVA with Bonferroni post hoc tests at a significant level of $p < 0.05$.

tion factor known to translocate into the nucleus from the cytoplasm upon ligand binding (Xu et al., 2002). We, therefore, performed immunofluorescence experiments to investigate PPARα nuclear accumulation in hCMEC/D3 upon activation with PPARα-specific ligands, clofibrate and GW7647. We observed approximately 34.8 and 31.67% increase in PPARα nuclear fluorescence intensity in cells treated with clofibrate (100 uM) or GW7647 (20 nM) compared with control (Fig. 3). These results suggest that the increase in PPARα nuclear accumulation could be mediated by an interaction with clofibrate or GW7647, two established PPARα ligands.

Ligand-Mediated Up-Regulation of ABCG2 mRNA in hCMEC/D3 Cells. We examined the mRNA expression of ABCG2 in hCMEC/D3 cells treated with PPARα ligands, clofibrate or GW7647, for 24 h. Both ligands significantly induced ABCG2 mRNA expression by approximately 71 and 49%, respectively compared with vehicle-treated control cells (Fig. 4). Our observations in hCMEC/D3 cells corroborate with previous findings where PPARα agonists (e.g., Wy14643, GW7647, and clofibrate) are reported to induce the mRNA expression of several drug transporters including Abcg2 in mouse liver and intestine (Moffit et al., 2006; Hirai et al., 2007). To evaluate whether the observed ABCG2 induction is mediated by PPARα, hCMEC/D3 cells were exposed to selective PPARα antagonists, MK886 (5 μM) or GW6471 (5 μM), in conjunction with the ligands for 24 h. MK886 and GW6471 are known to attenuate ligand-mediated activation of PPARα in other in vitro cell culture systems (Kehrer et al., 2001; Goto et al., 2011). As expected, addition of MK886 or GW6471 abolished ABCG2 mRNA induction mediated by clofibrate and GW7647 (Fig. 4).

Ligand-Mediated Up-Regulation of BCRP Protein Expression in hCMEC/D3 Cells. To determine whether the increase in ABCG2 mRNA expression resulted in changes in BCRP protein expression, hCMEC/D3 cells were cultured with increasing concentrations of clofibrate or GW7647 for 72 h. We observed a significant concentration-dependent up-regulation of BCRP protein in the presence ligands (Fig. 5, A and C). The highest induction of BCRP protein, approximately 175 and 125%, was observed when cells were incubated with 125 μM clofibrate or 20 nM GW7646, respectively. To assess the kinetics of BCRP protein expression induction, hCMEC/D3 cells were incubated with either clofibrate (100 μM) or GW7647 (20 nM) at several time points (6–72 h). As shown in Fig. 5, B and D, significant induction of BCRP protein expression was observed as early as 24 and 48 h of treatment with clofibrate and GW7647, respectively. The highest BCRP protein induction by both ligands (approximately 200%) was observed at 72 h (Fig. 5, B and D). It is noteworthy that we could not detect any significant increase in P-gp expression, another major ABC drug efflux transporter known to be expressed at the BBB by PPARα ligands in the cell culture system (data not shown).

Effect of PPARα Inhibitors on Ligand-Mediated BCRP Protein Induction. We further tested whether the observed BCRP protein induction is primarily mediated by PPARα in hCMEC/D3 cells exposed to varying concentrations of PPARα-specific antagonists (MK886 or GW6471) in conjunction with the ligands, clofibrate or GW7647, for 48 h. As expected, addition of MK886 (5 μM) with clofibrate (100 μM) or GW7647 (20 nM) decreased BCRP protein induction to nearly 0% (Fig. 6). Similar data were observed when another PPARα selective antagonist, GW6471, was used in a similar set of experiments (data not shown).

Effect of Clofibrate Treatment on BCRP Function in hCMEC/D3 Cells. To investigate whether the increase in

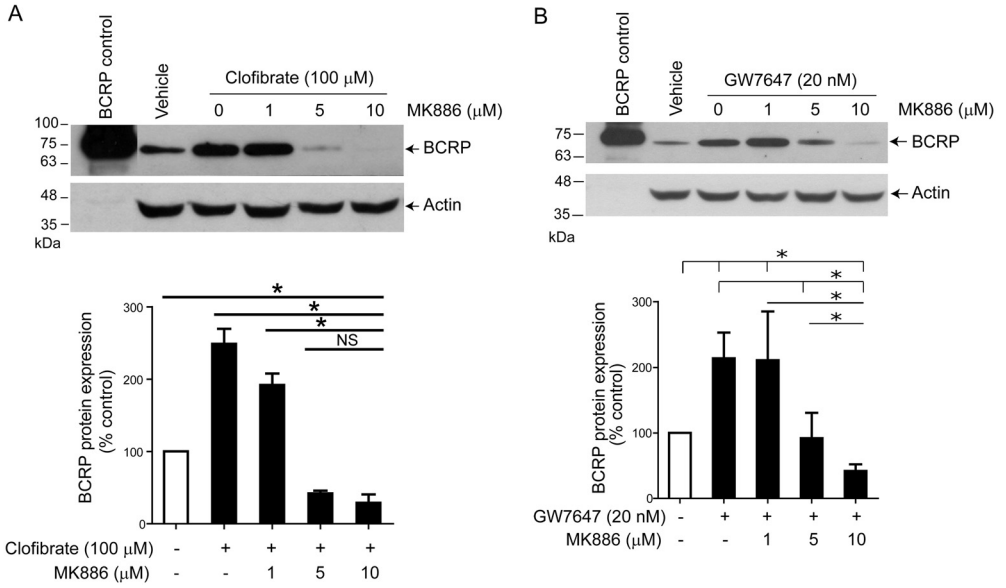

Fig. 6. Inhibition of BCRP protein induction by PPARα antagonists in hCMEC/D3 cells. BCRP protein expression was determined in hCMEC/D3 cells treated with PPARα ligands alone, clofibrate (100 μM)/GW7647 (20 nM), or in conjunction with clofibrate or GW7644 in the presence of different concentrations of PPARα antagonist, MK886 (1, 5, and 10 μM). A, representative immunoblot (top) and densitometric analysis (bottom) of BCRP expression in hCMEC/D3 cells exposed to vehicle, 100 μM clofibrate alone or 100 μM clofibrate in conjunction with 1, 5, or 10 μM MK886. B, representative immunoblot (top) and densitometric analysis (bottom) of BCRP expression in hCMEC/D3 cells exposed to vehicle, 20 nM GW7647 alone or 20 nM GW7647 in conjunction with 1, 5, or 10 μM MK886. Whole-cell lysates from hCMEC/D3 cells (50 μg/each) were resolved on a 10% SDS-PAGE gel and probed with anti-BCRP or anti-actin antibodies, respectively. The relative levels of BCRP expression were determined by densitometric analysis. Results are expressed as percentage change normalized to vehicle treated control (control) and reported as mean ± S.D. obtained from three independent experiments performed in cells pertaining to different passages. *, Statistically significant differences between treatment groups as determined by one-way ANOVA with Bonferroni post hoc tests at a significant level of $p < 0.05$.

protein expression resulted in a greater BCRP functional activity, we measured the accumulation of mitoxantrone, a chemotherapeutic agent and BCRP substrate, in hCMEC/D3 cells treated with clofibrate for 72 h. [^{3}H]Mitoxantrone accumulation was significantly reduced in cells treated with clofibrate compared with vehicle-treated control (5483 ± 435 pmol/mg protein versus 6270 ± 345 pmol/mg protein; $p < 0.05$). These data suggest that the higher level of BCRP expression in clofibrate treated cells is most likely associated with greater drug efflux activity resulting in lower levels of mitoxantrone accumulation by these cells. This effect was reversed in the presence of an established BCRP inhibitor, Ko143, in both vehicle- and clofibrate-treated cells, further confirming a BCRP-mediated efflux of mitoxantrone (Fig. 7).

Down-Regulation of BCRP Expression and Function by PPARα siRNA in hCMEC/D3 Cells. PPARα targeting siRNA was used to further examine the direct involvement of PPARα in the regulation of BCRP in hCMEC/D3 cells. In PPARα siRNA-transfected cells, PPARα protein expression was down-regulated by approximately 60%, whereas BCRP expression was reduced by nearly 23% as reflected by immunoblotting (Fig. 8, A and B) compared with cells treated with control scrambled siRNA. To investigate whether the decreased BCRP expression in PPARα siRNA-treated cells was associated with a lesser BCRP activity, we measured the accumulation of mitoxantrone in siRNA-transfected cells. Mitoxantrone accumulation was significantly higher in PPARα siRNA-treated cells compared with control siRNA-treated cells (8442 ± 610 pmol/mg protein versus 7752 ± 686 pmol/mg protein; $p < 0.05$), suggesting a lower BCRP function (Fig. 8C).

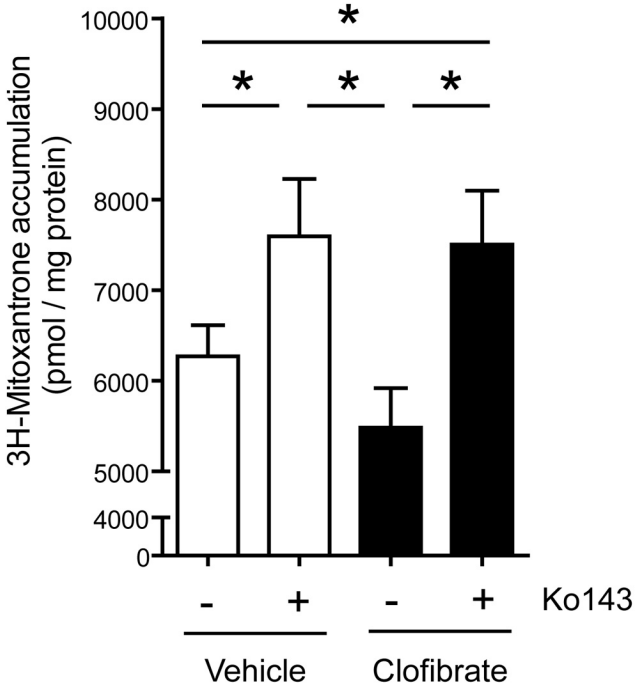

Fig. 7. Effect of clofibrate treatment on [^{3}H]mitoxantrone accumulation by hCMEC/D3 monolayer cells. Accumulation of 20 μM [^{3}H]mitoxantrone (2 h) was measured in the absence or presence of selective BCRP inhibitor Ko143, by hCMEC/D3 cells treated with either ethanol (vehicle) or clofibrate (100 μM) for 72 h. Results are expressed as mean percentage control ± S.E.M. of three separate experiments with each data point in an individual experiment representing triplicate measurements. Asterisks represent data points that are significantly different from control (*, $p < 0.05$).

Involvement of PPARα in the Transcriptional Regulation of *ABCG2* Gene in hCMEC/D3 Cells. Bioinformatics analyses of 5′-flanking region of human *ABCG2* promoter have identified a well conserved 150-bp region (−3946/−3796) containing three putative PPREs (Szatmari et al., 2006). We, therefore, hypothesized that PPARα binds to this region to mediate the induction of *ABCG2*. To test this hypothesis, we examined PPARα recruitment to this region in the native chromatin context by ChIP using specific anti-PPARα antibody previously validated in ChIP assays (Nagasawa et al., 2009). As shown in Fig. 9, an increased PPARα occupancy to the (−3946/−3796) region of *ABCG2* promoter was evident in hCMEC/D3 cells exposed to clofibrate for 3 h. PPARα occupancy was not increased in another region (−1527/−1268) of the same *ABCG2* promoter, suggesting the affinity of PPARα to the PPREs located at the −3946/−3796 region of *ABCG2* gene promoter. Similar observations were made with another PPARα ligand (GW7647) (data not shown).

Discussion

In addition to the well established role of PPARα in lipid metabolism, studies have suggested that PPARα could regulate the expression of transport proteins in the liver and intestine (Moffit et al., 2006; Hirai et al., 2007). However, at the BBB, the involvement of PPARα in the regulation of drug transporters is currently unknown. The objective of this study was to investigate the role of PPARα in the regulation of the drug efflux transporter, BCRP, expression, and function at the human BBB. Because of the challenge in obtaining healthy human brain samples and sufficient tissue, we used the hMEC/D3 cell culture system, an in vitro representative model of the human BBB (Weksler et al., 2005). When possible, human brain tissues and primary cultures of human brain microvessel endothelial cells were also used.

In this study, we detected PPARα protein expression and localization by Western blotting and immunofluorescence experiments in hCMEC/D3 cells (Fig. 1). An earlier report also documented PPARα expression in hMCEC/D3 cells by immunoblotting (Huang et al., 2009). In addition, we observed PPARα protein expression in primary cultures of human BBB-ECs and hFBTs (Fig. 2, A and B). These findings provide evidence that PPARα is expressed in human brain tissue and brain microvessel endothelial cells and can serve as a potential site for drug-receptor interactions and regulation of drug transporters and metabolic enzymes. PPARα has been reported to translocate into the cell nucleus upon ligand (fenofibrate) activation in human umbilical vein endothelial cells (Xu et al., 2002). Our results corroborate these data in hCMEC/D3 cells showing increased PPARα nuclear accumulation upon treatment with two different PPARα ligands, clofibrate and GW7647 further confirming the proposed mechanism of PPARs activation. Together, these observations provide the first evidence that PPARα is likely to be functional at the human BBB.

Previous studies have shown that PPARα ligands can induce *Bcrp* expression at the mRNA level in mouse intestine and liver (Moffit et al., 2006; Hirai et al., 2007). In the current study, we demonstrated that the earliest induction (approximately 49–72%) of ABCG2 mRNA occurred at 24 h after treatment of hMCEC/D3 cells by two different PPARα

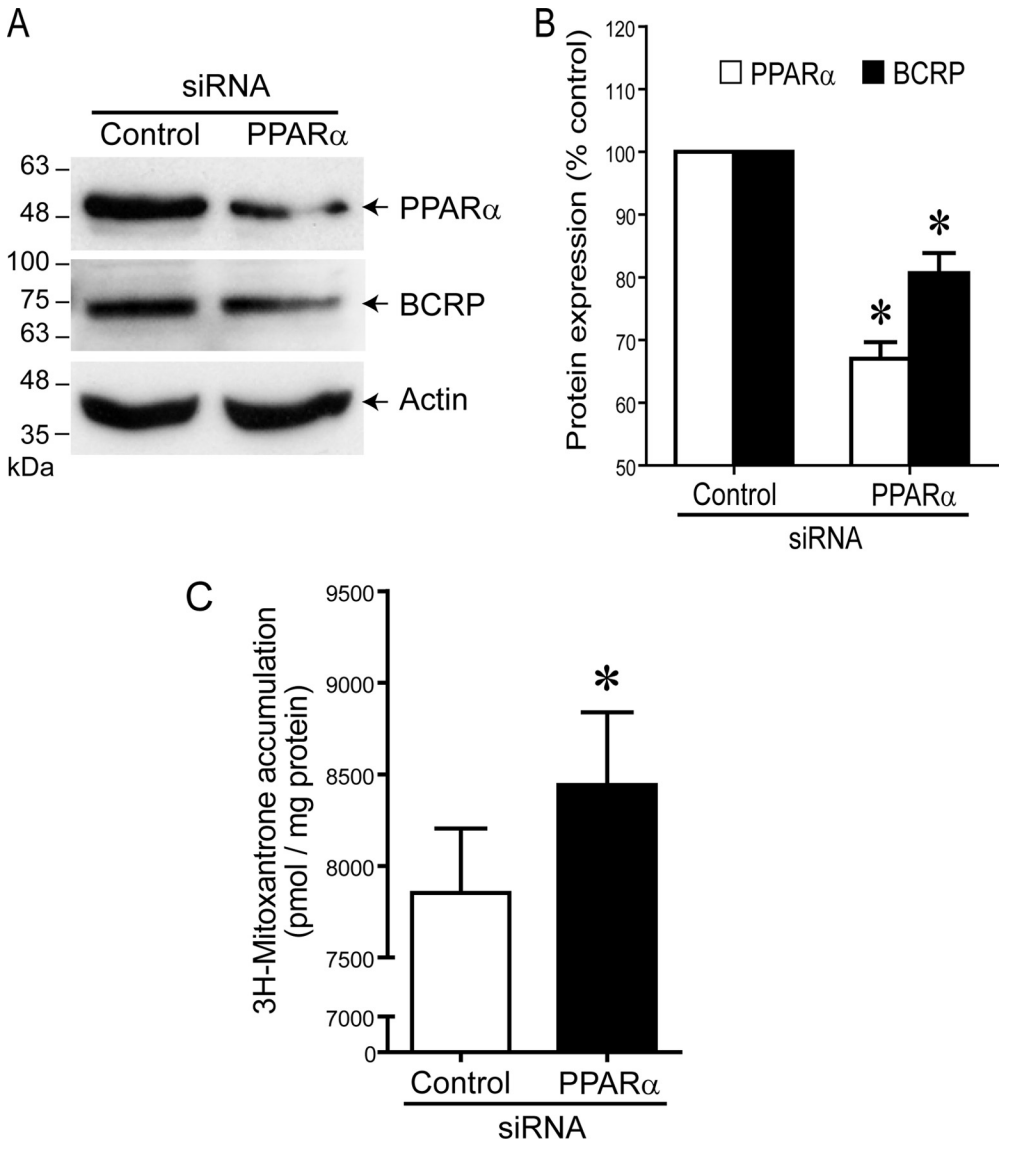

Fig. 8. Effect of PPARα down-regulation on BCRP protein expression and function in hCMEC/D3 cells. A, equal protein loading (50 μg/each) of homogenates derived from either control siRNA-treated hCMEC/D3 cells or cells treated with siRNA directed against PPARα were subjected to immunoblotting with anti-PPARα antibody (top). The blots were subsequently stripped and probed with anti-BCRP (middle) or anti-actin antibody as loading control (bottom). B, relative levels of PPARα and BCRP expression were determined by densitometric analyses. Results are expressed as percentage change normalized to control siRNA and reported as mean ± S.D. obtained from three independent experiments performed in cells pertaining to different passages. ∗, Statistically significant differences in BCRP and PPARα expression compared with control (control siRNA) were determined by two-tailed Student's *t* test with $p < 0.05$. C, accumulation of 20 μM [^{3}H]mitoxantrone (2 h) in hCMEC/D3 cells treated with either control siRNA or siRNA directed against PPARα. Results are expressed as mean percentage control ± S.E.M. of three separate experiments with each data point in an individual experiment representing triplicate measurements. Asterisks represent data points that are significantly different from control (∗, $p < 0.05$).

ligands. In addition, the PPARα antagonists, MK886 and GW6471, were able to attenuate the ligand-mediated ABCG2 mRNA induction. In addition to the induction of ABCG2 mRNA expression, PPARα ligands could also induce BCRP protein expression in a time- and concentration-dependent manner (approximately 100–200%), and these effects were attenuated by the PPARα-selective antagonists. Taken together, these observations strongly suggest for the first time that PPARα is involved in the regulation of BCRP at both the mRNA and the protein level in human brain microvessel endothelial cells.

In our transport experiments, we demonstrated significantly higher BCRP function in hCMEC/D3 cells treated with clofibrate compared with control. Similar trend was also observed in GW7647 treated cells. We further characterized the involvement of PPARα in the regulation of BCRP expression and function by using siRNA and observed reduced BCRP protein expression (over 20%) in hCMEC/D3 cells transfected with PPARα siRNA compared with control. Furthermore, significant higher mitoxantrone accumulation in PPARα siRNA treated cells was observed suggesting reduced BCRP function in the brain microvessel endothelial cells.

Applying the ChIP assay, we observed an enhanced PPARα binding to the −3946/−3796 region of the human *ABCG2* gene promoter in clofibrate-treated hCMEC/D3 cells. Similar enhancement is not seen in other regions (−1527/−1268) of the same *ABCG2* gene promoter reported to have no PPRE consensus (Szatmari et al., 2006). These data provide first evidence that PPARα can directly bind to the −3946/−3796 region of *ABCG2* gene promoter in hCMEC/D3 cells. A previous report identified three PPREs located at the −3946/−3796 region of the human *ABCG2* gene promoter for PPARγ, another PPAR isoform, binding in human dendritic cells (Szatmari et al., 2006). These findings further support the fact that PPAR receptors recognize a similar PPRE consensus for their binding to the target gene promoter.

The expression of BCRP is believed to be associated with the regulation of xenobiotic bioavailability, distribution, and toxicity in many tissues including the brain. Hence, the wide substrate specificity and tissue distribution of this transporter may play a major role in pharmacotherapy. Both endogenous (fatty acids, eicosanoids) and synthetic (lipid-lowering agents, insulin sensitizers) PPARα ligands are known to modulate PPARα activity. Drug efflux transporters such

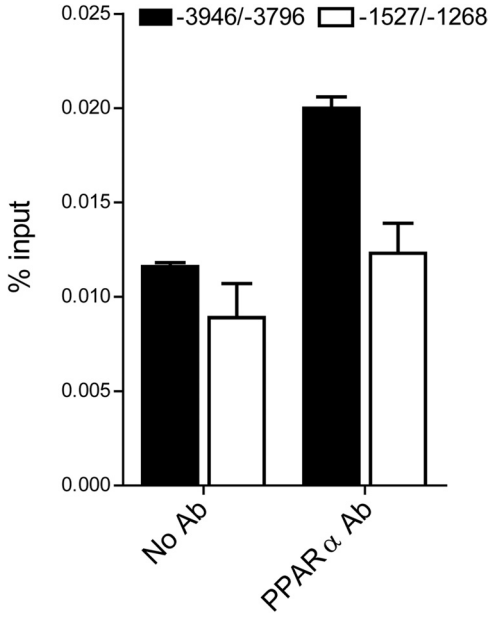

Fig. 9. Involvement of PPARα in the transcriptional regulation of *ABCG2* gene. ChIP was performed with anti-PPARα antibody (rabbit polyclonal) from hCMEC/D3 cells treated with clofibrate for 3 h. The precipitated DNA content was analyzed by qPCR using primers designed to amplify the PPRE-containing region of the ABCG2 gene promoter (−3946/−3796) or a nonspecific region of the same gene promoter (−1527/−1268). Results are shown as percentage of input DNA. As a negative control, no antibody control (No Ab) was used. All measurements were performed in triplicate. Data are the average of three independent experiments.

as BCRP and P-gp can serve as a major pathway for CNS drug clearance at the BBB and brain parenchyma where drug-metabolizing enzymes seem to be expressed at very low levels (Dauchy et al., 2008; Woodland et al., 2008). We propose that inhibiting PPARα activity can reduce BCRP functional expression rendering the BBB more permeable and potentially increasing the delivery of CNS drugs that are known BCRP substrates. On the other hand, activating PPARα can induce BCRP expression resulting in a less permeable barrier with increased protection against neurotoxins. Our data provide first evidence that the activity of PPARα in a human BBB model can be pharmacologically modulated by selective ligands (clofibrate, GW7647) or inhibitors (MK886, GW6471). This, in turn, could result in induction or down-regulation of BCRP expression and function in the brain.

In summary, in this work, we demonstrate the expression of PPARα in two in vitro representative systems of the human BBB, hCMEC/D3 and primary cultures of human brain-derived microvascular endothelial cells (BBB-ECs), as well as in hFBT samples. We also provide first evidence that pharmacological activation of PPARα can increase BCRP gene and protein expression as well as function in hCMEC/D3 cells and that this effect can be attenuated by specific PPARα inhibitors. In addition, we show that BCRP expression and function can be down-regulated by targeting PPARα using siRNA and demonstrate the ligand-induced PPARα binding to the PPREs in the BCRP promoter region, suggesting the direct involvement of PPARα in the regulation of this transport protein. As more xenobiotics are identified as ligands of PPARα, the selective tightening of the human BBB could be modulated by a careful design of drug regimens, which could improve CNS drug delivery or enhance neuroprotection.

Acknowledgments

We thank Dr. Pierre-Olivier Couraud (Institut Cochin, INSERM, Paris France) and Dr. Alexandre Prat (Hospitalier de l'Université de Montréal, Montréal, Canada) for kindly providing the HCMEC/D3 cell line system and cell pellets from primary cultures of human brain microvessel endothelial cells, respectively. We also thank Yu Yang for technical assistance.

Authorship Contributions

Participated in research design: Hoque and Bendayan.
Conducted experiments: Hoque and Robillard.
Contributed new reagents or analytic tools: Bendayan.
Performed data analysis: Hoque, Robillard, and Bendayan.
Wrote or contributed to the writing of the manuscript: Hoque and Bendayan.

References

Abbott NJ, Patabendige AA, Dolman DE, Yusof SR, and Begley DJ (2010) Structure and function of the blood-brain barrier. *Neurobiol Dis* **37:**13–25.
Bauer B, Hartz AM, Fricker G, and Miller DS (2004) Pregnane X receptor up-regulation of P-glycoprotein expression and transport function at the blood-brain barrier. *Mol Pharmacol* **66:**413–419.
Bauer B, Yang X, Hartz AM, Olson ER, Zhao R, Kalvass JC, Pollack GM, and Miller DS (2006) In vivo activation of human pregnane X receptor tightens the blood-brain barrier to methadone through P-glycoprotein up-regulation. *Mol Pharmacol* **70:**1212–1219.
Benani A, Krémarik-Bouillaud P, Bianchi A, Netter P, Minn A, and Dauça M (2003) Evidence for the presence of both peroxisome proliferator-activated receptors alpha and beta in the rat spinal cord. *J Chem Neuroanat* **25:**29–38.
Bendayan R, Lee G, and Bendayan M (2002) Functional expression and localization of P-glycoprotein at the blood brain barrier. *Microsc Res Tech* **57:**365–380.
Bendayan R, Ronaldson PT, Gingras D, and Bendayan M (2006) In situ localization of P-glycoprotein (ABCB1) in human and rat brain. *J Histochem Cytochem* **54:**1159–1167.
Bright JJ, Kanakasabai S, Chearwae W, and Chakraborty S (2008) PPAR regulation of inflammatory signaling in CNS diseases. *PPAR Res* **2008:**658520.
Chan GN, Hoque MT, Cummins CL, and Bendayan R (2011) Regulation of P-glycoprotein by orphan nuclear receptors in human brain microvessel endothelial cells. *J Neurochem* **118:**163–175.
Cullingford TE, Bhakoo K, Peuchen S, Dolphin CT, Patel R, and Clark JB (1998) Distribution of mRNAs encoding the peroxisome proliferator-activated receptor alpha, beta, and gamma and the retinoid X receptor alpha, beta, and gamma in rat central nervous system. *J Neurochem* **70:**1366–1375.
Dauchy S, Dutheil F, Weaver RJ, Chassoux F, Daumas-Duport C, Couraud PO, Scherrmann JM, De Waziers I, and Declèves X (2008) ABC transporters, cytochromes P450 and their main transcription factors: expression at the human blood-brain barrier. *J Neurochem* **107:**1518–1528.
Doyle LA, Yang W, Abruzzo LV, Krogmann T, Gao Y, Rishi AK, and Ross DD (1998) A multidrug resistance transporter from human MCF-7 breast cancer cells. *Proc Natl Acad Sci USA* **95:**15665–15670.
Enokizono J, Kusuhara H, Ose A, Schinkel AH, and Sugiyama Y (2008) Quantitative investigation of the role of breast cancer resistance protein (Bcrp/Abcg2) in limiting brain and testis penetration of xenobiotic compounds. *Drug Metab Dispos* **36:**995–1002.
Enokizono J, Kusuhara H, and Sugiyama Y (2007) Effect of breast cancer resistance protein (Bcrp/Abcg2) on the disposition of phytoestrogens. *Mol Pharmacol* **72:**967–975.
Goto T, Lee JY, Teraminami A, Kim YI, Hirai S, Uemura T, Inoue H, Takahashi N, and Kawada T (2011) Activation of peroxisome proliferator-activated receptor-alpha stimulates both differentiation and fatty acid oxidation in adipocytes. *J Lipid Res* **52:**873–884.
Hartz AM, Mahringer A, Miller DS, and Bauer B (2010) 17-β-Estradiol: a powerful modulator of blood-brain barrier BCRP activity. *J Cereb Blood Flow Metab* **30:**1742–1755.
Hirai T, Fukui Y, and Motojima K (2007) PPARalpha agonists positively and negatively regulate the expression of several nutrient/drug transporters in mouse small intestine. *Biol Pharm Bull* **30:**2185–2190.
Hoque MT and Ishikawa F (2001) Human chromatid cohesin component hRad21 is phosphorylated in m phase and associated with metaphase centromeres. *J Biol Chem* **276:**5059–5067.
Huang W, Eum SY, András IE, Hennig B, and Toborek M (2009) PPARalpha and PPARgamma attenuate HIV-induced dysregulation of tight junction proteins by modulations of matrix metalloproteinase and proteasome activities. *FASEB J* **23:**1596–1606.
Huang W, Rha GB, Han MJ, Eum SY, András IE, Zhong Y, Hennig B, and Toborek M (2008) PPARalpha and PPARgamma effectively protect against HIV-induced inflammatory responses in brain endothelial cells. *J Neurochem* **107:**497–509.
Ishikawa T (2009) The role of human ABC transporter ABCG2 (BCRP) in pharmacotherapy. *Adv Drug Deliv Rev* **61:**1–2.
Kehrer JP, Biswal SS, La E, Thuillier P, Datta K, Fischer SM, and Vanden Heuvel JP (2001) Inhibition of peroxisome-proliferator-activated receptor (PPAR)alpha by MK886. *Biochem J* **356:**899–906.
Kersten S, Desvergne B, and Wahli W (2000) Roles of PPARs in health and disease. *Nature* **405:**421–424.

Lee G, Babakhanian K, Ramaswamy M, Prat A, Wosik K, and Bendayan R (2007) Expression of the ATP-binding cassette membrane transporter, ABCG2, in human and rodent brain microvessel endothelial and glial cell culture systems. *Pharm Res* **24:**1262–1274.
Maliepaard M, Scheffer GL, Faneyte IF, van Gastelen MA, Pijnenborg AC, Schinkel AH, van De Vijver MJ, Scheper RJ, and Schellens JH (2001) Subcellular localization and distribution of the breast cancer resistance protein transporter in normal human tissues. *Cancer Res* **61:**3458–3464.
Miller DS (2010) Regulation of P-glycoprotein and other ABC drug transporters at the blood-brain barrier. *Trends Pharmacol Sci* **31:**246–254.
Moffit JS, Aleksunes LM, Maher JM, Scheffer GL, Klaassen CD, and Manautou JE (2006) Induction of hepatic transporters multidrug resistance-associated proteins (Mrp) 3 and 4 by clofibrate is regulated by peroxisome proliferator-activated receptor alpha. *J Pharmacol Exp Ther* **317:**537–545.
Muerhoff AS, Griffin KJ, and Johnson EF (1992) The peroxisome proliferator-activated receptor mediates the induction of CYP4A6, a cytochrome P450 fatty acid omega-hydroxylase, by clofibric acid. *J Biol Chem* **267:**19051–19053.
Nagasawa M, Hara T, Kashino A, Akasaka Y, Ide T, and Murakami K (2009) Identification of a functional peroxisome proliferator-activated receptor (PPAR) response element (PPRE) in the human apolipoprotein A-IV gene. *Biochem Pharmacol* **78:**523–530.
Pardridge WM (2010) Biopharmaceutical drug targeting to the brain. *J Drug Target* **18:**157–167.
Polgar O, Robey RW, and Bates SE (2008) ABCG2: structure, function and role in drug response. *Expert Opin Drug Metab Toxicol* **4:**1–15.
Robyr D, Wolffe AP, and Wahli W (2000) Nuclear hormone receptor coregulators in action: diversity for shared tasks. *Mol Endocrinol* **14:**329–347.
Ronaldson PT, Ashraf T, and Bendayan R (2010) Regulation of multidrug resistance protein 1 by tumor necrosis factor alpha in cultured glial cells: involvement of nuclear factor-kappaB and C-Jun N-terminal kinase signaling pathways. *Mol Pharmacol* **77:**644–659.
Ronaldson PT, Persidsky Y, and Bendayan R (2008) Regulation of ABC membrane transporters in glial cells: relevance to the pharmacotherapy of brain HIV-1 infection. *Glia* **56:**1711–1735.
Schachtrup C, Emmler T, Bleck B, Sandqvist A, and Spener F (2004) Functional analysis of peroxisome-proliferator-responsive element motifs in genes of fatty acid-binding proteins. *Biochem J* **382:**239–245.
Szatmari I, Vámosi G, Brazda P, Balint BL, Benko S, Széles L, Jeney V, Ozvegy-Laczka C, Szántó A, Barta E, et al. (2006) Peroxisome proliferator-activated receptor gamma-regulated ABCG2 expression confers cytoprotection to human dendritic cells. *J Biol Chem* **281:**23812–23823.
Vlaming ML, Lagas JS, and Schinkel AH (2009) Physiological and pharmacological roles of ABCG2 (BCRP): recent findings in Abcg2 knockout mice. *Adv Drug Deliv Rev* **61:**14–25.
Wang X, Hawkins BT, and Miller DS (2011) Aryl hydrocarbon receptor-mediated up-regulation of ATP-driven xenobiotic efflux transporters at the blood-brain barrier. *FASEB J* **25:**644–652.
Wang X, Sykes DB, and Miller DS (2010) Constitutive androstane receptor-mediated up-regulation of ATP-driven xenobiotic efflux transporters at the blood-brain barrier. *Mol Pharmacol* **78:**376–383.
Weksler BB, Subileau EA, Perrière N, Charneau P, Holloway K, Leveque M, Tricoire-Leignel H, Nicotra A, Bourdoulous S, Turowski P, et al. (2005) Blood-brain barrier-specific properties of a human adult brain endothelial cell line. *FASEB J* **19:**1872–1874.
Woodland C, Huang TT, Gryz E, Bendayan R, and Fawcett JP (2008) Expression, activity and regulation of CYP3A in human and rodent brain. *Drug Metab Rev* **40:**149–168.
Xu X, Otsuki M, Sumitani S, Saito H, Kouhara H, and Kasayama S (2002) RU486 antagonizes the inhibitory effect of peroxisome proliferator-activated receptor alpha on interleukin-6 production in vascular endothelial cells. *J Steroid Biochem Mol Biol* **81:**141–146.
Zastre JA, Chan GN, Ronaldson PT, Ramaswamy M, Couraud PO, Romero IA, Weksler B, Bendayan M, and Bendayan R (2009) Up-regulation of P-glycoprotein by HIV protease inhibitors in a human brain microvessel endothelial cell line. *J Neurosci Res* **87:**1023–1036.

Address correspondence to: Dr. Reina Bendayan, Department of Pharmaceutical Sciences, Leslie Dan Faculty of Pharmacy, University of Toronto, 144 College St., Toronto, ON, M5S 3M2, Canada. E-mail: r.bendayan@utoronto.ca